J Mater Sci: Mater Med (2010) 21:1343–1351
DOI 10.1007/s10856-009-3876-0

Silk fibroin/chitosan–hyaluronic acid versus silk fibroin scaffolds for tissue engineering: promoting cell proliferations in vitro

Tze-Wen Chung · Yu-Lin Chang

Received: 15 May 2009 / Accepted: 17 September 2009 / Published online: 5 February 2010

Abstract The feasibility of silk fibroin protein (SF) scaffolds for tissue engineering applications to promote cell proliferation has been demonstrated, as well as the ability to mimic natural extra-cellular matrix (ECM), SF/chitosan (CS), a polysaccharide, scaffolds for tissue engineering. However, the response of cells to SF/CS–hyaluronic acid (SF/CS–HA) scaffolds has not been examined, which this study attempts to do and then compares those results with those of SF scaffolds. SF/CS–HA microparticles were fabricated to produce scaffolds in order to examine the proliferations of human dermal fibroblasts (HDF) in the scaffolds. Positive zeta potentials and ATR-FTIR spectra confirmed the co-existence of SF and CS–HA in SF/CS–HA microparticles. HDF proliferated well and migrated into SF/CS–HA scaffolds for around 160 μm in depth, as well as those in SF scaffolds after 7 days of cultivation, as observed using confocal microscopy. Interestingly, HDF grown in SF/CS–HA scaffolds had a markedly higher cell density than that in SF ones. Additionally, MTT assay revealed that the growth rates of HDF in SF/CS–HA scaffolds significantly exceeded ($P < 0.01$, $n = 5$) those in scaffolds of SF and SF/CS. The daily glucose consumptions and lactate formations, metabolic parameters, of HDF grown in SF/CS–HA and SF/CS scaffolds were significantly higher ($P < 0.01$, $n = 3$) than those in SF ones in most culturing days. Results of this study suggest that SF/CS–HA scaffolds have better cell responses for tissue engineering applications than SF ones.

T.-W. Chung (✉) · Y.-L. Chang
Department of Chemical and Material Engineering, National Yunlin University of Science and Technology, Dou-Liu, Yun-Lin 640, Taiwan, ROC
e-mail: twchung@yuntech.edu.tw

1 Introduction

Silk fibroin (SF) from silkworms, *Bombyx mandarina* cocoons, is structurally characterized as natural block copolymers comprising hydrophobic blocks with a repetitive sequence of short side-chain amino acids such as glycine and alanine, as well as hydrophilic blocks with highly complex sequences that are composed of both larger side-chain amino acids and charged amino acids, which have been extensively studied for tissue engineering applications [1–4]. According to those studies, the antigenic properties of SF are associated with sericin. Following the removal of sericin, SF films have weaker inflammatory responses in vivo than films fabricated using collagen or polylactide (PLA) [1–3]. Membranes of SF or SF scaffolds have been examined recently to explore their potentials in tissue engineering applications such as in repairing bones [4], ligaments [5] and skins [6, 7]. Positive responses of mesenchymal stem cells (MSCs) cultured in SF mats or sponges to the regeneration of bone and cartilage tissue engineering have also been shown [4, 5].

Notably, polysaccharides and proteins significantly impact living cells and tissue growth. Interactions between these biopolymers in an extra-cellular matrix (ECM) form macromolecular structures by association [8]. Therefore, in addition to enhancing the mechanical properties of SF scaffolds due to formation of hydrogen bonds between SF and CS, incorporating CS into SF to produce SF/CS films or three dimensional SF/CS scaffolds can also promote cell adhesion and proliferation in the aforementioned films or scaffolds [9–12].

CS, an amino polysaccharide derived from chitin via de-acetylation, is a biodegradable and biocompatible material containing numerous reactive groups, including amine groups. CS or CS modified with various active

molecules for fabricating films or scaffolds has been thoroughly investigated for tissue engineering applications [13–15] or for use as a drug delivery vehicle [16]. Since the structure of CS resembles that of glycosaminoglycan (GAG) in an ECM, it has been incorporated into SF in order to fabricate SF/CS films or scaffolds for potential tissue engineering applications [9–12]. Alternatively, hyaluronic acid (HA), a water-soluble poly-saccharide, is distributed throughout ECM of all connective tissues in humans and other mammals [17]. As is well known, HA can promote cell migration, and is frequently used as scaffolds for cartilage tissue engineering and wound healing [18, 19]. However, to our knowledge, incorporating CS–HA into SF to produce SF/CS–HA scaffolds for tissue engineering has not been investigated. Therefore, this study examines whether SF/CS–HA scaffolds can further promote cellular growth, as tested by using human dermal fibroblasts (HDF). Those results are then compared with those of SF scaffolds as a control group. CS–HA are co-sprayed with SF to produce SF/CS–HA micro-particles mixed with salts, processed by mechanical pressing, genipin crosslinking, glycine inhibition reactions and desalted in de-ionized water to produce SF and SF/CS–HA scaffolds with a high porosity. The responses of the cells to SF/CS–HA scaffolds are compared with SF and SF/CS (for a reference) ones by examining HDF grown in those scaffolds through use of a confocal microscopy and viability assay after 7 days of cultivation. Moreover, daily glucose consumptions and lactate formations during HDF cultured in scaffolds are examined to elucidate primary metabolic activities. The potentials of SF/CS–HA scaffolds for tissue engineering are explored as well.

2 Materials and methods

2.1 Preparation of SF and SF/CS–HA microparticles

Bombyx mandarina cocoons were purchased from a silk center in Taiwan (ShihTan, Miaoli, Taiwan). The SF solutions were prepared as described elsewhere [20, 21]. Briefly, silk cocoons were boiled for 30 min in 0.02 M Na_2CO_3, and, then, rinsed thoroughly in distilled water to extract the glue-like sericin proteins. The extracted SF were then dissolved in 9.3 M LiBr solution at 60°C for 4 h, yielding a 20% (w/v) solution [1], which was then dialyzed against distilled water using a dialysis membrane (MWCO 6000) (Pierce, USA) at room temperature for 48 h to remove the salt. The final concentration of the SF aqueous solution was 8% (w/v). Next, this concentration was determined by weighing the residual solid in a known solution volume after drying at 60°C for 24 h. Chitosan (96% de-acetylated; MW, 200 kDa) (Sigma–Aldrich, USA) was dissolved with 1% acetic acid (99.8% Sigma–Aldrich, USA) and, then, added into a previously purified SF solution (1.5% w/v) for preparing SF/CS solutions. For SF/CS–HA solution, hyaluronic acid (HA) (MW, 15 kDa) (Lifecore, USA) was added into the SF/CS solution prior to being fabricated microparticles. The final concentrations for SF/CS and SF/CS–HA solutions were SF-to-CS-to-HA (w/w/w) ratios of 10:1:0 and 10:1:1, respectively.

The SF, SF/CS–HA and SF/CS microparticles were initially fabricated using a spray-drying machine (EYERS SD-1000, Tokyo Rikakikai Co., Tokyo, Japan) at 120°C, under a 20 KPa tip pressure, airflow rate of 0.65 m^3/min and solution flow rate of 20 ml/min. The microparticles diameter of each SF-base particle was calculated by examining the images of particles of scanning electron microscopy (SEM) to determine their diameters. One hundred of SF-base microparticles were counted per batch and, then, three different batches of the same SF-base particles were counted. The fabricated SF-based microparticles had diameters of 3–8 μm. The particles were immersed in 95% alcohol for several hours followed by air drying for subsequent applications.

2.2 Surface characterization of SF-based hybrid microparticles

The zeta potentials of SF, SF/CS–HA and SF/CS microparticles in the aqueous solution were determined at 25°C using a device for measuring the zeta potential (Zeta Plus 90 Particle Sizer) (Brookhaven Instruments Co., USA) with a 5 mW He–Ne laser ($\lambda = 633$ nm). Transmission spectra of the SF, SF/CS–HA and SF/CS microparticles in KBr pellets were then determined using an ATR-FTIR analyzer with a resolution of 2 cm^{-1}, and analyzed utilizing the built-in standard software package Perkin–Elmer Spectrum One (Perkin–Elmer Co., Norwalk, CT, USA). Finally, the static water contact angles of the SF, CS, HA, SF/CS–HA and SF/CS films were determined by adding 40 μl distilled water to their surfaces and using a contact angle meter (Edmund Industry Optics, Japan) equipped with a charge-coupled device (CCD) recorder (Sanyo, Japan).

2.3 Preparation of SF and SF/CS–HA scaffolds

SF and SF/CS–HA microparticles were mixed with NaCl particles of 106–305 μm particle sizes with various ratios of 1–13 and, then, pressed using a pressing machine at a pressure of 5 GPa at room temperature to produce scaffolds. These SF, SF/CS–HA and SF/CS scaffolds were then crosslinked in 1% genipin (Challenge Bio-products Co., Ltd., Taipei, Taiwan) solution for 12 h at 45°C; the crosslinking reactions were terminated by adding 3% glycine at 25°C for more than 12 h. Following glycine

treatment, the SF-based scaffolds were immersed and stirred in distilled water to remove residual glycine for several hours. Moreover, the scaffolds were further immersed in distilled water for dissolving salts to produce a high porosity of scaffolds. These dark-blue scaffolds had a diameter of 13 mm, thickness of 1 mm, and mass of 20–25 mg with the swelling ratio of 15–20% (swelling ratio (%) = (wet weight − dry weight)/dry weight × 100%). To prepare SF/CS scaffolds for experiments in this study, the preparation procedures were the same as SF/CS–HA ones.

The porosity of a silk scaffold was determined using liquid displacement. In this study, nitrogen was used as the displacement liquid as it permeates through silk scaffolds without swelling or shrinking the matrix. According to earlier studies, the porosity of a scaffold was determined by the following equation [22]: $\varepsilon = (V_T - (W/\rho))/V_T$; where ε, W, V_T and ρ refer to the porosity, the weight and total volume of the scaffold, and the material density of the scaffolds, respectively. Determining the material density of a scaffold by a fully automatic density meter (AccuPyc1330 Pycnometer density analyzer, Micomeri Aics, USA) involves first immersing the scaffolds into a known volume of nitrogen and then calculating the amounts of nitrogen absorbed into scaffolds, followed by determination with a meter. The surface morphology of the SF and SF hybrid scaffolds were examined via scanning electron microscopy (SEM) according to the procedures in our earlier study [23]. The interior structures of scaffolds were observed by freezing SF-based scaffolds in liquid nitrogen, through use of a razor blade to cut the frozen scaffolds. Samples were sputter coated with gold. Finally, the morphology of the scaffolds was observed with a field emission gun SEM (HITACHI S4800-1, Tokyo, Japan) [15, 24].

2.4 Culturing of HDF and cell proliferation in SF/CS–HA scaffolds

For HDF cultivation, SF, SF/CS–HA and SF/CS scaffolds with a thickness of 1 mm were sterilized at 120°C and rinsed with cultural medium-106 (Cascade Biologics Inc., USA) several times. The scaffolds were then placed into a 24-well cultural plate for seeding HDF and conducting a culture study. Detailed procedures for cell cultivation, including HDF in various biomaterials, can be found elsewhere [24]. In general, cryopreserved human dermal fibroblasts (HDF) were obtained from Cascade Biologics Inc. (Lot #: C-003-5C, Portland, Oregon, USA). A vial of cryopreserved HDF purchased from the same company was first thawed in a 37°C water bath. The number of cells in the vial were counted using a hematocytometer and then diluted to a concentration of 2.0×10^4 viable cells/ml in cell culture flasks with a surface area of 25 cm^2 (Costar, Corning Life Sciences, Acton, MA, USA.) containing medium-106 (Cascade Biologics Inc., USA) supplemented with 2% fetal bovine serum, 10 ng/ml of fibroblast growth factor and 1% of an antibiotic (Cascade Biologics Inc., USA) as subcultures for use in the subsequent cell culture to yield a new cycle of HDF [24].

For growing cells in those scaffolds, aforementioned harvested HDF of third to seventh cycles of subcultures at 1.0×10^6 viable cells/ml were seeded onto the scaffolds and cultured at 37°C with 5% CO_2/95% air with a relative humidity of 80%; the cultural medium was refreshed daily for 7 days. Following culturing, the proliferation of HDF in the scaffolds by a confocal microscopy was observed by staining proteins and nuclei of HDF with various reagents. To do so, the scaffolds were initially fixed by 10% formaldehyde (Sigma–Aldrich, USA) and blocked in 2% bovine serum albumin (BSA) (Sigma–Aldrich, USA)/Phosphate Buffered Saline (PBS) (Applied Biosystems, CA, USA). Next, anti-vimentin (mouse IgG anti-rat in ratio of 1:200, Chemicon, CA, USA) with appropriate secondary antibodies (Alexa Fluor 488 secondary antibody, Molecular Probes, Invitrogen, USA) matching with the primary antibodies were utilized for HDF staining. Additionally, negative controls were used in each analysis to eliminate the interference of the primary or secondary antibody. The stained HDF in the scaffolds were counterstained with a Hoechst 33342 (Invitrogen, USA) for visualizing their nuclei. The stained HDF in the scaffolds were observed by radiating excitation wavelengths at 488 and 561 nm via a laser confocal scanning microscopy (LCSM) (Zeiss Inverted LSM410, Zeiss Optical Company, Germany).

2.5 Viability and metabolic parameters assay of HDF cultured in SF/CS–HA scaffolds

The viability of HDF cultured on various scaffolds was determined by thiazolyl blue assay (MTT reagent) (Sigma–Aldrich, USA) using a slight modification of the Mosmann method [25]. To perform the assay, the HDF cultured in SF-based scaffolds for 7 days were trypsinized with 1 ml trypsin (trypsin/EDTA solution 1X, sterile, Cascade Biologics, USA) three times; they were then detached from the scaffolds. The suspensions containing HDF were centrifuged ($1500 \times g$) to collect the cells for MTT assay. The procedures for MTT assay were the same as in our earlier studies [24, 26]. (Briefly, OR In brief,) 300 µl MTT solution was incubated with the HDF cells at 37°C for 4 h and, then, 0.5 ml dimethyl sulfoxide solution (DMSO, Sigma Chemicals, USA) was added to dissolve formazan crystals The absorbencies of formazan solutions were determined at 630–570 nm using an ELISA micro-plate reader (EL × 800) (Bio-Tek Instruments, Inc., VT, USA). An attempt was also made to balance the effects of various

weights of the scaffold on cellular growth, in which the absorbance values of the formazan solution were determined for the HDF grown in SF and the hybrid scaffolds were divided by the weight of each scaffold [27].

The metabolic conditions of HDF in the scaffolds during culturing were analyzed by collecting and determining glucose and lactate concentrations of used cultural medium through use of a glucose kit (Glucose assay kit, Sigma, USA) and a lactate kit (Lactate reagent set enzymatic method, Instruchemie, Netherlands), as described in other studies [28]. In general, 2 ml of used cultural medium were mixed with 4 ml perchloric acid (8%) to precipitate proteins after 10 min of centrifugation (1500×g). The supernatants were collected for determining the concentrations of glucose and lactate. The glucose concentration was determined by reacting 0.2 ml of suspensions with 1 ml of the glucose reagent at 37°C for 15 min, and the suspension was (determined OR measured OR evaluated) by a UV/VIS spectrometer (Jasco UV-530, Kobe, Japan) at a wavelength of 340 nm. Next, lactate formations were determined by reacting 0.1 ml suspensions with 2.9 ml of lactate reagent at 37°C for 15 min, and the suspension was determined by a UV/VIS spectrometer at a wavelength of 340 nm.

All calculations of this study were performing using Sigmastat statistical software (Jandel Science Corp., San Rafael, CA, USA). Statistical significance in the Student's t-test corresponded to a confidence level of at minimum 95%. Data are presented as mean ± SD of measurements in triplicate. Differences were considered statistically significant at $P < 0.05$.

3 Results and discussion

3.1 (Characteristics OR attributes OR properties OR features) of SF/CS–HA microparticles

Figure 1a shows the SEM micrographs of surface morphologies for SF/CS–HA microparticles. Irregular shapes of SF microparticles fabricated by a spray-dried method resembled those found in other studies [29]. Additionally, the morphologies of SF/CS–HA and SF/CS microparticles did not differ from those of SF microparticles (data not shown). Interestingly, the zeta potentials of microparticles varied markedly. For instance, those of SF, SF/CS–HA and SF/CS microparticles were −14.6 ± 1.4 mV, 1.2 ± 3.6 mV and 10.0 ± 1.6 mV ($n = 4$), respectively. Since the amine groups of CS were protonized in a weak acid solution, CS is responsible for the positive zeta potentials of SF/CS and SF/CS–HA microparticles [30]. Notably, the decreasing positive zeta potential of SF/CS–HA microparticles was attributed to the presence of HA in microparticles. Figure 1b schematically depicts three-dimensional SF/CS–HA scaffolds with a porosity of 91.7%. The SF/CS–HA microparticles and salts were packed by mechanical pressing, crosslinking by genipin, glycine inhibition process and finally desalting in D.I. water to fabricate the scaffolds.

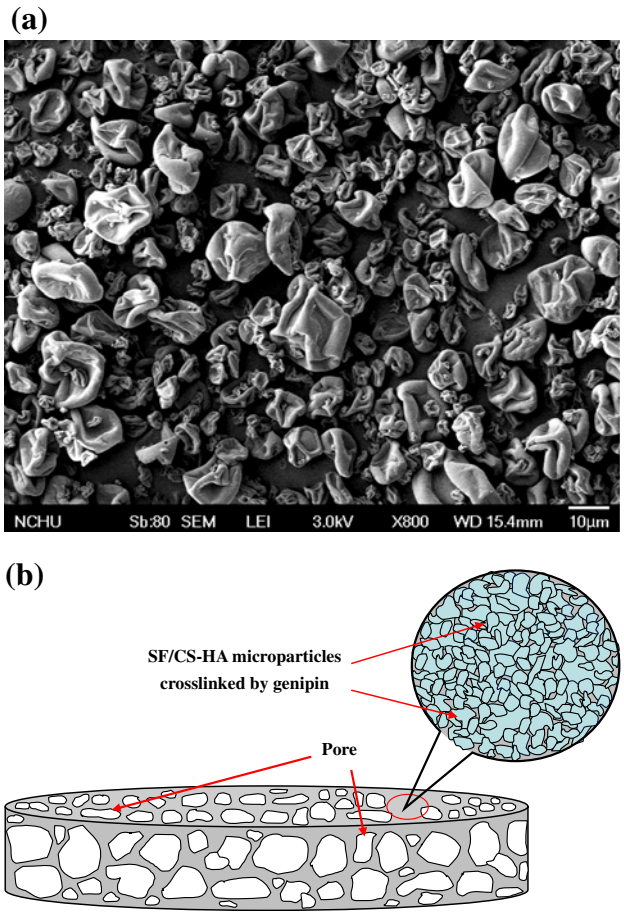

Fig. 1 (**a**) The SEM micrographs of SF/CS–HA microparticles for fabricating the scaffolds and those of SF and SF/CS microparticles are about the same as the SF/CS–HA ones. (**b**) The schematic diagram for three-dimension SF/CS–HA scaffolds with porosity of 91.7% and mean size of pores of 200 μm for HDF culturing. According to our observation in SEM micrographs, the structures of SF/CS–HA scaffolds are about the same as those of SF and SF/CS ones

The constituents of SF/CS–HA microparticles were characterized by performing ATR-FTIR analysis. The ATR-FTIR spectra of SF microparticles in the β-sheet included strong absorption peaks appearing at 1650 cm^{-1} (amide I), 1530 cm^{-1} (amide II), and 1233 cm^{-1} (amide III) which is attributed to the combination of N–H in-plane bending and C–N stretching vibration of peptide [31] (Fig. 2). Chitosan had absorption bands appearing at 1543 cm^{-1} and 1645 cm^{-1}, corresponding to the amine groups. In SF/CS microparticles, although new peaks did not appear after the reaction, the structural changes, which were attributed to genipin cross-linking, can be revealed by

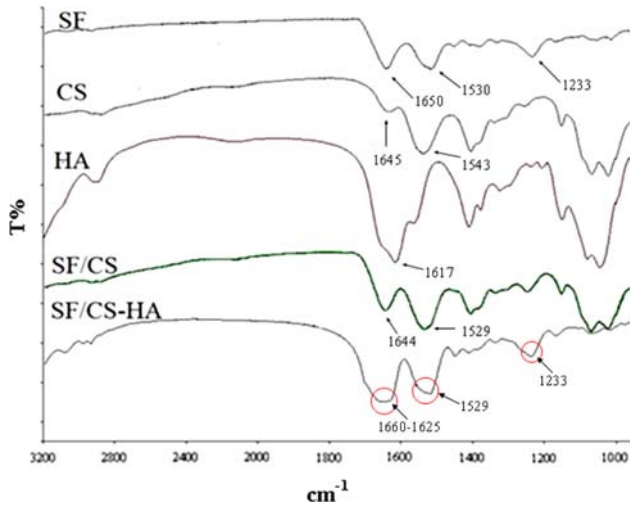

Fig. 2 ATR-FTIR transmission spectra of SF, CS, HA, SF/CS and SF/CS–HA microparticles. The characteristic peaks of incorporating CS and CS–HA into SF microparticles are shown on SF/CS and SF/CS–HA curves, respectively

an analysis of amides I (CO, stretching), II (N–H deformation), and III (C–N stretching and N–H deformation) in the spectra. Comparing spectra of SF with SF/CS reveals that the amide I (1644 cm^{-1}) and amide II (1529 cm^{-1}) bands of the later one shift to low wave numbers. Those bands also appeared for SF/CS microparticles, and a similar band was identified in another study [30]. Notably, HA contains abundant carboxylic acids in which a strong absorption band appears at 1617 cm^{-1}, which was observed for SF/CS–HA microparticles. Since interactions among carboxylic groups of SF and amine groups of CS result in the conformational transition of SF, absorption bands of the amide groups of SF and CS shifted to 1644 cm^{-1} for SF/CS and SF/CS–HA microparticles. Moreover, SF/CS–HA microparticles had one broad bands appearing in the range of 1625–1660 cm^{-1}, as attributed to interaction among N–H of CS, amide I of SF [32] and carbonyl groups of HA.

3.2 SEM morphology of high porosity of SF/CS–HA scaffolds

Scaffolds with a high porosity were fabricated by mixing various ratios of NaCl particles with SF/CS–HA microparticles such as 1: 9, as well as various sizes of NaCl particles such as 106–305 μm with the microparticles, followed by mechanical pressing to fabricate solid scaffolds. Experimental results indicated that size of salts slightly affected the porosity of the scaffolds (data not shown). For this study, the size of 106–305 μm NaCl particles was selected to fabricate high porosity of SF/CS–HA scaffolds. In contrast, various ratios of SF/CS–HA microparticles to NaCl particles significantly affected the porosity of the scaffolds (Table 1). Accordingly, the ratio of SF/CS–HA microparticles to NaCl particles was set at 1:13 to produce scaffolds with a high porosity (91.1 ± 1.7%, $n = 5$) which had a mean size of pores of 200 μm and in a range of 100–350 μm of pores. Figure 3 shows the SEM morphologies of internal structures of SF/CS–HA scaffolds fabricated by the above conditions. According to this figure, the scaffolds were constructed by many large compartments, resulting from the salts, with many small pores in the walls of compartments to connect different compartments. The small pores in the walls might be attributed to SF-based microparticles might detach from the compartments because of incompletely crosslinking between the microparticles in the interiors of the fabricated scaffolds of this study. Additionally, the same morphologies of internal structures of SF and SF/CS scaffolds were observed as those of SF/CS–HA scaffolds (data not shown). Notably, various ratios of salt contents to microparticles, as well as genipin crosslinking conditions to prepare the scaffolds, dominated the internal structures such as their porosities and pore dimensions.

Table 1 The porosities of scaffolds were function of the ratios of the weight of SF/CS–HA microparticles to that of NaCl particles

Size of NaCl particles: 106–305 μm	
Weight ratios of SF/CS–HA microparticles and NaCl particles	Porosity (%)
1:7	82.1 ± 1.2
1:9	84.3 ± 1.0
1:11	88.0 ± 1.0
1:13	91.7 ± 1.7

The weight ratio of SF/CS–HA microparticles to NaCl particles of 1:13 was selected for fabricating the scaffolds. The same ratio was applied to the SF scaffolds

3.3 Proliferations of HDF in SF/CS–HA, SF/CS and SF scaffolds observed by confocal microscopy

Figure 4a–c show the proliferations of HDF in SF, SF/CS and SF/CS–HA scaffolds were observed by confocal microscopy via vimentin, an immuno-histochemical staining, and nuclei staining of HDF with various depths after 7 days of culturing. As is well known, vimentin is the major subunit protein of the intermediate filaments of cytoskeleton of cells. In this study, the morphology of HDF was observed using vimentin staining of HDF. For instance, according to the images of the confocal microscope (magnification at 100×), the spindle shape in vimentin distribution of cytoplasm of HDF (in green) and their nucleus (in blue) were observed, indicating that the well-grown HDF was proliferated in an interior region of

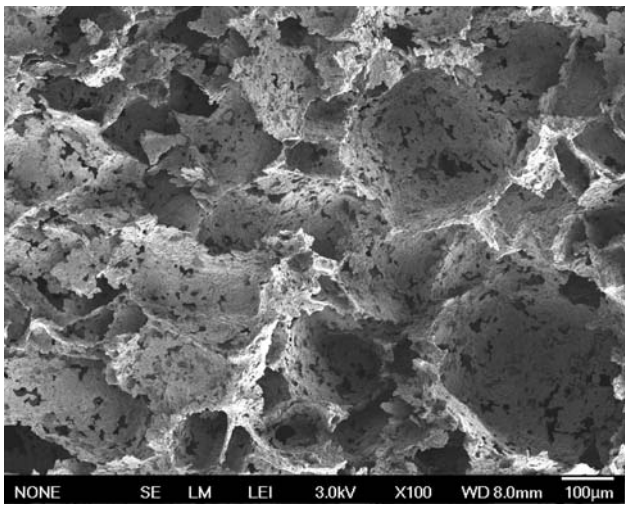

Fig. 3 The SEM micrograph for the morphology an interior structure of SF/CS–HA scaffolds with porosity of 91.1 ± 1.7% which had mean size of pores of 200 µm and in range of 100–350 µm of pores. In addition, the scaffold contains a lot of small pores that may interconnect different compartments. SF and SF/CS scaffolds had similar micrographs (data not shown)

those scaffolds. According to the three dimensional images of cells in SF scaffolds versus the depth of the images taken by a confocal microscope, HDF could be distributed in a region from the surface to 160 µm in the depth of interior of the scaffolds (Fig. 4a). This is despite the fact that the images were disturbed partially by the un-filtered, strong green fluorescent radiated by the backbone of the scaffolds (Fig. 4a). According to three dimensional images of cells taken from SF/CS–HA scaffolds (Fig. 4b), HDF proliferated and distributed in the same region of SF/CS–HA scaffolds as those in SF ones. Interestingly, comparing Fig. (4a, b) after semi-quantitatively calculating their cell densities reveals that cell density of HDF grown in SF/CS–HA scaffolds (Fig. 4b) was significantly exceeded that in SF ones (Fig. 4a). Additionally, Fig. 4c shows the distributions of various colors of nucleus of HDF, colorization by the software of the microscope versus the various depths of SF/CS–HA scaffolds (e.g., from blue to red colors, indicating that cells were distributed from the surface to 140 µm depth of SF/CS–HA scaffolds, respectively). Most of the cell population proliferated in the region of 50–80 µm depths within SF/CS–HA scaffolds. For comparison, according to Fig. 4d, the major populations of cells proliferated in SF/CS scaffolds were nearly the same as those in SF/CS–HA ones. Interestingly, according to the semi-quantitative calculations, the density of HDF that proliferated in SF/CS–HA scaffolds (Fig. 4c) was markedly exceeded that in SF/CS scaffolds (Fig. 4d). We postulate that the high porosities of the scaffolds (e.g., about 91%) containing many compartments with interconnect pores (Fig. 3) contribute to the proliferation and migration of HDF into interior regions of all scaffolds. Nevertheless, the hybrid CS–HA with SF to fabricate the scaffolds promotes the proliferation rates of HDF in scaffolds more than the SF and SF/CS scaffolds do. However, further study is warranted to elucidate the detailed mechanisms such as conformational changes of SF by adding CS–HA in order to increase the proliferation and migration of HDF in SF/CS–HA scaffolds, respectively (Fig. 4b, c).

3.4 Viability and metabolic parameters assay of HDF cultured in SF/CS–HA scaffolds

Owing to its ability to reveal the extent of cellular metabolism and viability of the cells [27, 33], MTT assay has been extensively adopted to evaluate the proliferation rates of cells in biomaterials [15, 26, 27]. Using the same assay, this study analyzed the proliferation rates of HDF in SF, SF/CS–HA and SF/CS (for comparisons) scaffolds [26, 27]. Interestingly, the proliferation rates of HDF in SF/CS–HA scaffolds significantly exceeded ($P < 0.05$ or better, $n = 5$) those in SF and SF/CS scaffold (Fig. 5) after 7 days of culturing. For instance, the formazan absorption value for HDF in SF scaffolds was 0.033 ± 0.001 (Abs/mg scaffold), which was significantly lower than that in SF/CS–HA ones (0.043 ± 0.002, (Abs/mg scaffold), $n = 5$). Previous studies have indicated that SF scaffolds increase adhesion and growth of several cells, including osteoblasts [4, 21, 34] and mesenchymal stem cells [4, 5, 35, 36]. In this design, incorporating CS–HA to SF as biomaterials for producing SF/CS–HA scaffolds facilitated the proliferations of HDF in SF/CS–HA scaffolds compared with SF ones, as illustrated by cell images and MTT viability assay. Interestingly, the MTT values of cells measured for SF/CS–HA scaffolds were significantly higher than those of SF/CS ones (Fig. 5). As is well known, HA that promotes cell migration mediated by CD44 [17] and structurally affects the SF conformations (e.g., increasing formations of β-sheet) in scaffolds [10, 13, 37] may contribute to the proliferation and MTT viability results (Figs. 4, 5).

3.5 Determination of metabolic parameters of HDF cultured in SF, SF/CS SF/CS–HA scaffolds

Previous studies have indicated that the primary metabolic parameters, daily glucose consumptions and lactate formation, are important factors to observe the status of a cell cultured in 3-D scaffolds or bioreactors [27, 28]. Therefore, to determine those parameters, this study investigated the metabolic status of HDF in SF/CS–HA, SF and SF/CS scaffolds during 7 days of cultivation. Figure 6 shows the concentrations of daily glucose consumptions and lactate formations in a supernatant of HDF cultured in various scaffolds as a function of time. Interestingly, the

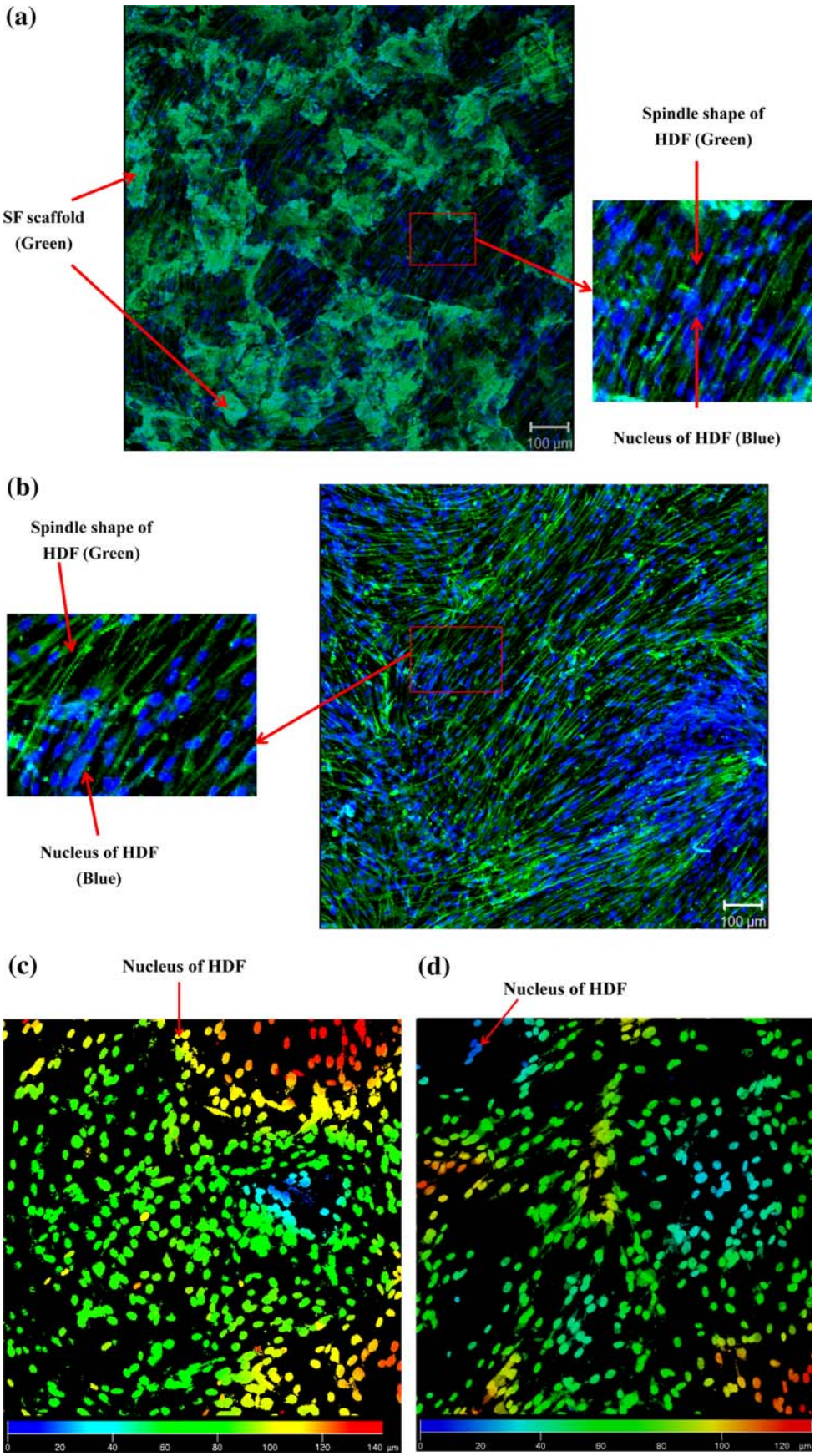

Fig. 4 The morphology of nucleus (blue) and vimentin (green) staining HDF grown in the scaffolds after 7 days of culturing, taken by a confocal microscope with a magnification at 100×, Bars = 100 μm. The maximum observed depths for HDF proliferation in (**a**) SF, (**b**) SF/CS–HA scaffolds were all 160 μm inside the scaffolds, respectively. The spindle shapes of HDF (by vimentin staining) were clearly observed in all of the scaffolds. (**c**) and (**d**) presented the distributions of the nucleus of HDF presented in various colors verse the observed depths of SF/CS–HA (143 μm) and SF/CS (129 μm) scaffolds, respectively, (e.g., from blue to red colors, indicating from the surface to 140 μm depth of SF/CS–HA scaffolds) with a magnification at 200×

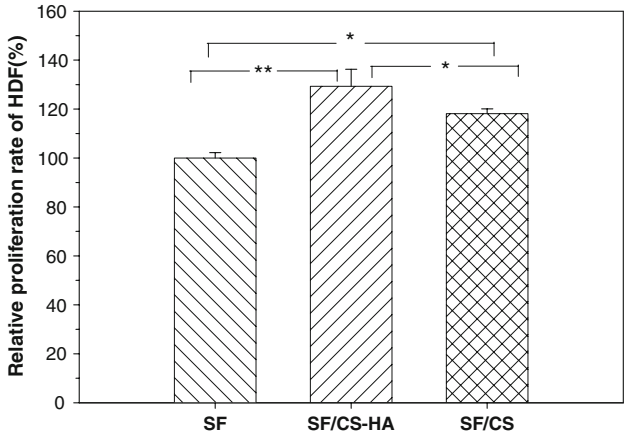

Fig. 5 The relative proliferation rates of HDF cultured in SF (control group, the MTT value of this group is assigned as 100%), SF/CS–HA and SF/CS (for a reference) scaffolds for 7 days. The proliferation rate of HDF cultured SF/CS–HA scaffolds were significantly higher than those in SF/CS and SF ones, respectively (* $P < 0.05$; ** $P < 0.01$; Data presented are mean ± S.D., $n = 5$)

concentrations of consumptions of glucose for HDF cultured in SF/CS–HA scaffolds were significantly higher ($P < 0.01$, $n = 3$) than those in SF scaffolds during most of days of cultivation (Fig. 6). Moreover, the concentrations of formations of lactate for HDF cultured in SF/CS–HA hybrid scaffolds were significant higher ($P < 0.01$, $n = 3$) than those in SF scaffolds during most of days of cultivation. Hence, the higher concentrations in consumptions of glucose and formations of lactate (Fig. 6) indicated that the growth and proliferation rates of HDF in SF/CS–HA scaffolds would exceed those in SF scaffolds during culturing. Notably, the assay results of metabolic

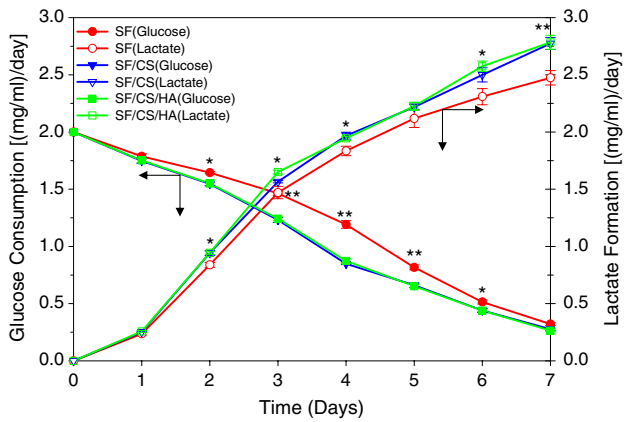

Fig. 6 The metabolic parameters, the concentrations of daily glucose consumptions and lactate formations in supernatant were determined for HDF proliferated in SF SF/CS and SF/CS–HA scaffolds for 7 days. Generally, HDF proliferated in SF/CS–HA scaffolds had significant higher concentrations of daily glucose consumptions and lactate formations (* $P < 0.05$; ** $P < 0.01$, $n = 3$) than SF scaffolds in most of time during culturing while there was less different between SF/CS–HA and SF/CS groups

parameters in the supernatant of SF/CS–HA scaffolds during HDF cultivations (Fig. 6) corresponded to those of MTT viability assay of cell proliferation in the same scaffolds at the end of culturing (Fig. 5). However, the values of metabolic parameters for SF/CS and SF/CS–HA scaffolds only slightly differed from each other during culturing. Since the factors to affect HDF proliferated in scaffolds are complicated, the detailed mechanism such as different compositions or pore distributions of fabricated scaffolds in this study to affect the metabolisms of HDF in those scaffolds still needed to be explored.

4 Conclusions

This study investigated whether incorporating CS–HA into SF would affect in vitro proliferations of HDF versus SF only by fabricating high porosities of SF and SF/CS–HA scaffolds. Comparing the proliferation rates of HDF in SF/CS–HA scaffolds with SF revealed that the proliferation rates of HDF in HA containing scaffolds significantly exceeded those in SF and SF/CS ones (Figs. 4, 5) for 7 days of culturing. Results of this study suggest that the SF/CS–HA scaffolds are highly promising for tissue engineering applications versus SF ones.

Acknowledgements The authors would like to thank the National Science Council of the Republic of China, Taiwan, for financially supporting this research under Contract Nos; NSC-96-2321-B-002-043, NSC-97-2314-B-002-045 and NSC-96-2221-E-224-077-MY3.

References

1. Vepari C, Kaplan DL. Silk as a biomaterial. Prog Polym Sci. 2007;32:991–1007.
2. Yanagisawa S, Zhu Z, Kobayashi I, Uchino K, Tamada Y, Tamura T. Improving cell-adhesive properties of recombinant *Bombyx mori* silk by incorporation of collagen or fibronectin derived peptides produced by transgenic silkworms. Biomacromolecules. 2007;8(11):3487–92.
3. Panilaitis B, Altman GH, Chen J, Jin HJ, Karageorgiou V, Kaplan DL. Macrophage responses to silk. Biomaterials. 2003;24(18):3079–85.
4. Vepari C, Jin HJ, Kim HY, Kaplan DL. Electrospun silk-BMP-2 scaffolds for bone tissue engineering. Biomaterials. 2006;27(16):3115–24.
5. Fan H, Liu H, Toh SL, Goh JC. Enhanced differentiation of mesenchymal stem cells co-cultured with ligament fibroblasts on gelatin/silk fibroin hybrid scaffold. Biomaterials. 2008;29(8):1017–27.
6. Unger RE, Peters K, Wolf M, Motta A, Migliaresi C, Kirkpatrick CJ. Endothelialization of a non-woven silk fibroin net for use in tissue engineering: growth and gene regulation of human endothelial cells. Biomaterials. 2004;25(21):5137–46.
7. Sugihara A, Sugiura K, Morita H, Ninagawa T, Tubouchi K, Tobe R. Promotive effects of a silk film on epidermal recovery from full-thickness skin wounds. Proc Soc Exp Biol Med. 2000;225(1):58–64.

8. Kardestuncer T, McCarthy MB, Karageorgiou V, Kaplan D, Gronowicz G. RGD-tethered silk substrate stimulates the differentiation of human tendon cells. Clin Orthop Relat Res. 2006;448:234–9.
9. Cai K, Rechtenbach A, Hao J, Bossert J, Jandt KD. Polysaccharide-protein surface modification of titanium via a layer-by-layer technique: characterization and cell behaviour aspects. Biomaterials. 2005;26(30):5960–71.
10. Gobin AS, Froude VE, Mathur AB. Structural and mechanical characteristics of silk fibroin and chitosan blend scaffolds for tissue regeneration. J Biomed Mater Res A. 2005;74:324–34.
11. Engbers-Buijtenhuijs P, Buttafoco L, Poot AA, Dijkstra PJ, De Vos RAI, Sterk LM, et al. Silk fibroin/chitosan scaffold: preparation, characterization, and culture with HepG2 cell. J Mater Sci Mater Med. 2008;19(12):3545–53.
12. Silva SS, Motta A, Rodrigues MT, Pinheiro AF, Gomes ME, Mano JF. Novel genipin-cross-linked chitosan/silk fibroin sponges for cartilage engineering strategies. Biomacromolecules. 2008;9(10):2764–74.
13. Lanza RP, Langer R, Vancanti J, editors. Principles of tissue engineering. 2nd ed. San Diego, CA: Academic Press; 2000.
14. Martino AD, Sittinger M, Risbud MV. Chitosan: a versatile biopolymer for othopaedic tissue-engineering. Biomaterials. 2005;26(10):5983–90.
15. Chung TW, Wang YZ, Pan CI, Wang SS, Fu Eur. Poly (ε-caprolactone) grafted with chitosan enhances growth of human fibroblasts—effects of different degree of surface nano-roughness. J Mater Sci Mater Med. 2009;20:397–404.
16. Chung TW, Wang SS, Tsai WJ. Accelerating thrombolysis with chitosan-coated plasminogen activators encapsulated in poly-(lactide-co-glycolide) (PLGA) nanoparticles. Biomaterials. 2008;29(2):228–37.
17. Gross-Jendroska M, Lui GM, Song MK, Stern R. Retinal pigment epithelium-stromal interactions modulate hyaluronic acid deposition. Invest Ophthalmol Vis Sci. 1992;33(12):3394–9.
18. Yoo HS, Lee EA, Yoon JJ, Park TG. Hyaluronic acid modified biodegradable scaffolds for cartilage tissue engineering. Biomaterials. 2005;26(14):1925–33.
19. Dechert TA, Ducale AE, Ward SI, Yager DR, Dechert TA, Ducale AE, et al. Hyaluronan in human acute and chronic dermal wounds. Wound Repair Regen. 2006;14(3):252–8.
20. Inoue S, Tanaka K, Arisaka F, Kimura S, Ohtomo K, Mizuno S. Silk fibroin of *Bombyx mori* is secreted, assembling a high molecular mass elementary unit consisting of H-chain, L-chain, and P25, with a 6:6:1 molar ratio. J Biol Chem. 2000;275(51):40517–28.
21. Karageorgiou V, Tomkins M, Fajardo R, Meinel L, Snyder B, Wade K. Porous silk fibroin 3-D scaffolds for delivery of bone morphogenetic protein-2 in vitro and in vivo. J Biomed Mater Res A. 2006;78(2):324–34.
22. Kim UJ, Park J, Kim HJ, Wada M, Kaplan DL. Three- dimensional aqueous-derived biomaterial scaffolds from silk fibroin. Biomaterials. 2005;26:2775–85.
23. Lin YS, Wang SS, Chung TW, Wang YH, Chiou SH, Hsu JJ, et al. Growth of endothelial cells on different concentrations of Gly-Arg-Gly-Asp photochemically grafted in polyethylene glycol modified polyurethane. Artif Organs. 2001;25(8):617–21.
24. Chung TW, Wang YZ, Huang YY, Pan CI, Wang SS. Poly (ε-caprolactone) grafted with nano-structured chitosan enhances growth of human dermal fibroblasts. Artif Organs. 2006;30(1):35–41.
25. Gerlier D, Thomasset N. Use of MTT colorimetric assay to measure cell activation. J Immunol Methods. 1986;94(1–2):57–63.
26. Chung TW, Yang MG, Liu DZ, Chen WP, Pan CI, Wang SS. Enhancing growth human endothelial cells on Arg-Gly-Asp (RGD) embedded poly (ε-caprolactone) (PCL) surface with nanometer scale of surface disturbance. J Biomed Mater Res A. 2005;72(2):213–9.
27. Jin HJ, Chen J, Karageorgiou V, Altman GH, Kaplan DL. Human bone marrow stromal cell responses on electrospun silk fibroin mats. Biomaterials. 2004;25(6):1039–47.
28. Dhiman HK, Ray AR, Panda AK. Three-dimensional chitosan scaffold-based MCF-7 cell culture for the determination of the cytotoxicity of tamoxifen. Biomaterials. 2005;26(9):979–86.
29. Yeo JH, Lee KG, Lee YO, Kim SY. Simple preparation and characteristics of silk fibroin microsphere. Eur Polym J. 2003;29:1195–9.
30. She Z, Jin C, Huang Z, Zhang B, Feng Q, Xu Y. Silk fibroin/chitosan scaffold: preparation, characterization, and culture with HepG2 cell. J Mater Sci Mater Med. 2008;19(12):3545–53.
31. Garside P, Lahlil S, Wyeth P. Characterization of historic silk by polarized attenuated total reflectance Fourier transform infrared spectroscopy. Appl Spectrosc. 2005;59(10):1242–7.
32. Chen X, Li WJ, Zhong W, Lu Y, Yu TY. pH sensitivity and ion sensitivity of hydrogels based on complex-forming chitosan/silk fibroin interpenetrating polymer network. J Appl Polym Sci. 1997;65:2257–62.
33. Mosmann T. Rapid colorimetric assay for cellular growth and survival: application to proliferation and cytotoxicity assays. J Immunol Methods. 1983;65(1–2):55–63.
34. Meinel L, Fajardo R, Hofmann S, Langer R, Chen J, Snyder B. Silk implants for the healing of critical size bone defects. Bone. 2005;37(5):688–98.
35. Marolt D, Augst A, Freed LE, Vepari C, Fajardo R, Patel N. Bone and cartilage tissue constructs grown using human bone marrow stromal cells, silk scaffolds and rotating bioreactors. Biomaterials. 2006;27(36):6138–49.
36. Hofmann S, Knecht S, Langer R, Kaplan DL, Vunjak-Novakovic G, Merkle HP. Cartilage-like tissue engineering using silk scaffolds and mesenchymal stem cells. Tissue Eng. 2006;12(10):2729–38.
37. Garcia-Fuentes M, Giger E, Meinel L, Merkle HP. The effect of hyaluronic acid on silk fibroin conformation. Biomaterials. 2008;29(6):633–42.